COVER SHEET

TITLE: Predicting and Interpreting the Hofmeister Effects of Different Salts with Nucleic Base

AUTHOR'S NAME: Runyu Hong

MAJOR: Biochemistry

DEPARTMENT: Biochemistry

MENTOR: Professor M. Thomas Record, Jr.

DEPARTMENT:

MENTOR(2):

DEPARTMENT(2):

YEAR: 2016

(The following statement must be included if you want your paper included in the library's electronic repository.)

The author hereby grants to University of Wisconsin-Madison the permission to reproduce and to distribute publicly paper and electronic copies of this thesis document in whole or in part in any medium now known or hereafter created.

ABSTRACT

Predicting and Interpreting the Hofmeister Effects of Different Salts with Nucleic Bases and Aromatic Compounds Using Solubility Assay

The interaction between salts and nucleic acid bases or aromatic compounds plays an important role in noncovalent biopolymer assembly processes such as DNA and RNA helix formation and protein-nucleic acid interactions. The project determines effects of five salts contains Hofmeister ions (NaF, KBr, KSCN, NH_4Cl, NH_4Br) on the solubility of 11 model compounds (nucleic bases, nucleic base derivatives, and naphthalene) to experimentally quantify salt-model compound preferential interactions (chemical potential derivatives designated μ_{23}). Values of μ_{23} are obtained from the derivative of the logarithm of the model compound solubility with respect to the molal concentration of salt. These data are analyzed to predict interactions of these Hofmeister salts with the five functional groups of nucleic acid bases (aromatic C and N; carbonyl O; Sp3 N, aliphatic C). The results are used to predict the interactions between Hofmeister salts and other organic compounds and effect of Hofmeister salts on nucleic acid processes.

Runyu Hong/Biochemistry
Author Name/Major

Runyu Hong
Author Signature

12/15/16
Date

M Thomas Record/Biochemistry
Mentor Name/Department

Tom Record
Mentor Signature

Predicting and Interpreting the Hofmeister Effects of Different Salts with Nucleic Bases and Aromatic Compounds Using Solubility Assay

by

Runyu Hong

Under the Direction of

Professor M. Thomas Record, Jr., Departments of Biochemistry and Chemistry

Senior Honors Thesis

Dec 12th, 2016

I have supervised this work, read this thesis and certify that it has my approval.

12/14/16 — Date

Tom Record — Thesis Advisor's Signature

ABSTRACT

The interaction between salts and nucleic acid bases or aromatic compounds plays an important role in noncovalent biopolymer assembly processes such as DNA and RNA helix formation and protein-nucleic acid interactions. The project determines effects of five salts contains Hofmeister ions (NaF, KBr, KSCN, NH_4Cl, NH_4Br) on the solubility of 11 model compounds (nucleic bases, nucleic base derivatives, and naphthalene) to experimentally quantify salt-model compound preferential interactions (chemical potential derivatives designated μ_{23}). Values of μ_{23} are obtained from the derivative of the logarithm of the model compound solubility with respect to the molal concentration of salt. These data are analyzed to predict interactions of these Hofmeister salts with the five functional groups of nucleic acid bases (aromatic C and N; carbonyl O; Sp3 N, aliphatic C). The results are used to predict the interactions between Hofmeister salts and other organic compounds and effect of Hofmeister salts on nucleic acid processes.

INTRODUCTION

Background and Significance

Salts can affect the stability of biomolecules through two types of interactions: the Coulombic interactions, which involve formation of atmosphere of hydrated salt ions around the hydrated charged groups of biomolecules, and the ion-specific Hofmeister effects, which are due to the competition between different ions and water to interact with the functional groups of the biomolecules. When the concentration of salt is below 0.1M, Coulombic effect usually dominates; at higher salt concentrations, especially greater than 1.0M, Coulombic interactions are reduced and specific interactions between uncharged biopolymer surfaces and salt ions have a dominant effect.

Noncovalent and weak covalent interactions, including Van der Waal's forces, hydrogen bonding, dipole-dipole interactions, and hydrophobic effect, play important roles in stabilizing most of the cellular fundamental structures such as protein folds, DNA double helix, and lipid bilayers. These assemblies are governed by the thermodynamics that is a sensitive function of the conditions of the solution. The dissolved components such as salts and organic metabolites have direct impact on the biopolymers' conformations.

Hofmeister effects describe the favorable and unfavorable interactions between proteins and salts on biopolymer processes[1]. In 1888, protein scientist Franz Hofmeister discovered the effects of a series of salt ions on protein solubility (Figure 1)[2]. In dissolving and also in unfolding proteins, the change of water accessible protein surface area (ΔASA) is positive since surfaces

buried in the solid form or in the folded state are exposed. Salt ions that interact favorably with these protein surfaces will solubilize and unfold the protein, while the ions that interact unfavorably with these protein surfaces will precipitate and fold the protein.

Anions: $SO_4^{2-} > F^- > Cl^- > Br^- > NO_3^- > I^- > ClO_4^- > SCN^-$

Cations: $NR_4^+ > Na^+ \cong K^+ > Li^+ > NH_4^+ > > GuH^+$

Precipitating ⟷ Solubilizing

Disfavor ΔASA>0 Favor ΔASA>0

Figure 1. Hofmeister series, ranked by ability of ions to disfavor or favor biopolymer processes that expose biopolymer surface to water (ΔASA>0).

The reason why different Hofmeister salts have different impact on protein's stability is because of the interactions between ions and functional groups of the protein. When the protein is denatured, the functional groups that are normally buried inside during folded state are exposed to the solution. If the ion interacts favorably with these exposed functional groups, then this salt ion will destabilize the protein from its native folded structure. Thermodynamic analysis reveals that these destabilizing salts lower the free energy of the denatured protein comparing to the absence of the salts and to the folded form at the same salt concentration, which makes the unfolding state more favorable. Not only protein folding process, but also a large variety of biopolymer processes, including enzyme activity, protein stability, micelle formation, hydrocarbon solubility, optical rotation of amino acids, DNA methylation, melting, synthesis, and the formation of an air-water interface[1,3,4,5,6], have been found to respond to changes in salt concentration in a manner consistent with Hofmeister's anion and cation series from protein solubility measurements. It has been studied both experimentally and computationally, yet still

not fully understood[7,8]. The preferential interactions (μ_{23}) between the salts and model compounds or biopolymers are quantified by the derivative of the chemical potential of the model compound or biopolymer with respect to the molal concentration of the salt[7,8].

$$\mu_{23} = d\mu_2/dm_3 \quad (1)$$

A negative μ_{23} shows a favorable interaction, indicating that the salt ions out-compete water to interact with the model compound, while a positive μ_{23} indicates an unfavorable interaction, which means water out-competes ion to interact with the compound[8].

The effect of Hofmeister salts on biopolymer processes are determined by measuring the equilibrium concentration quotient (K_{obs}) as a function salt concentration (m_3). Typically, $\ln K_{obs}$ varies linearly with m_3. The derivative (slope) of $\frac{\partial \ln K_{obs}}{\partial m_3}$ is related to the free energy derivative called the salt *m*-value, as shown in Equation 2-1[9]. In this equation, the component 1, 2, and 3 stands for water, biopolymer surfaces, and the solutes of interest respectively. For solubility studies, where K_{obs} equals to m_2, we can relate m-value and $\Delta\mu_{23}$ by Equation 2-2. In this paper, biopolymer surfaces are the surface of model compounds (nucleobases and aromatic compounds) and the solute of interest one of the 5 Hofmeister salts respectively.

$$\text{m-value} = \frac{d\Delta G^{\circ}_{obs}}{dm_3} = \frac{-RTdlnK_{obs}}{dm_3} \qquad (2\text{-}1)$$

$$\text{m-value} = \frac{-RTdlnm_2{}^{ss}}{dm_3} = \left(\frac{d\mu_2}{dm_3}\right)_{m_2} = \Delta\mu_{23} \quad (2\text{-}2)$$

One-way Analysis

To interpret the $\Delta\mu_{23}$ value, we dissect the interaction into additive contributions of

interactions between salt and individual functional group on the base[1,10]. In Equation 3, ASA_i is the water accessible area of the functional group i on the nucleobase[11], α_i is the "interaction potential" that measures the strength of the interaction of the salt with individual surface type i on the base. The SurfaceRacer Program calculated the water accessible surface areas of each functional group on the base surface and the values are listed in Appendix section[12]. In this ASA-based analysis, the model compound is divided into five different surface types (five types of functional groups): aromatic C; aromatic N; carbonyl O; Sp3 N, and aliphatic C. α_i values are interaction strengths of the solute with unit area of each of these functional groups.

$$\frac{\mu_{23}}{RT} = \sum_i \alpha_i \cdot ASA_i \qquad (3)$$

After getting the preferential interactions, the interpretation of the observed α_i values is based on the solute partitioning model (SPM)[13].

Through Eq. 4-1 and Eq. 4-2 α_i values can be related to a local-bulk partition coefficient (K_p). Eq. 4-1 is applied for nonelectrolyte solutions whereas Eq. 4-2 is applied for electrolyte solutions. The Kp value describes the constant ratio of concentration in molality of salt in the local area versus that in the bulk solution; b_1 is the amount of hydration water per $Å^{-2}$ (here we used 0.18 H_2O per $Å^{-2}$); the concentration of water in dilute solution is 55.5 mol/Kg[13]. To study the specific ion-base interactions, Eq. 4-2 can be used, which features the calculation of $K_{p,x}$. $K_{p,x}$ can be associated with $K_{p,3}$ by Eq. 4-3. v_+ and v_- stand for the number of ions in one unit of salt, and v is the total number of ions present in one unit of salt. The conversion of salt activity derivative to salt concentration derivative involves the term $v(1+\varepsilon_{\pm})$, which is

experimentally determined from and equals to $dOsm/dm_3$[14].

$$\alpha_i = -\frac{(K_{p,3} - 1)b_1(1+\varepsilon)}{55.5} \tag{4-1}$$

$$\alpha_i = -\frac{vb_1(1+\varepsilon_{\pm})}{55.5}\left(\frac{v_+K_{p,+} + v_-K_{p,-}}{v} - 1\right) \tag{4-2}$$

$$vK_{p,3} = v_+K_{p,+} + v_-K_{p,-} \tag{4-3}$$

The salts (NaF, KBr, KSCN, NH_4Cl, and NH_4Br) to be studied in this project complement other salts ($(GuH)_2SO_4$, GuHCl, GuHSCN, Na_2SO_4, NaCl, NaSCN) that our laboratory has previously investigated, and provide significant information about why natural selection favored salts of K^+ and anionic amino acids like glutamate and aspartate instead of instead of NH_4^+ or GuH^+ salts or inorganic anions like Cl^- or Br^- as the prevalent salts in growing cells. Combining the data set of this project and previous projects mentioned above, interaction difference between different cations can also be determined by comparing salts with the same anion (eg. Na^+ vs. K^+ by comparing KSCN with previous data of NaSCN) and vice versa. Eleven nucleic bases and aromatic compounds (Figure 2) are used as model compounds for the solubility test of each salt. These model compounds contain five common functional groups: aromatic C, aromatic N, carbonyl O, Sp3 N, and aliphatic C, which allows us to dissect interactions into the contribution of each structural component.

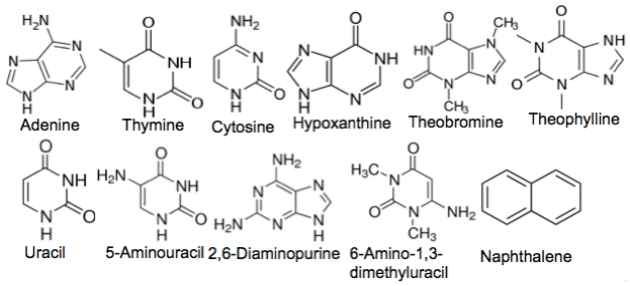

Figure 2. 11 model compounds that are nucleic bases, nucleic bases' derivatives, and related aromatic compounds.

Application

Quantified alpha values are used to predict interactions between the 5 salts and other organic compounds. Comparisons between our predicted results and published experimental data can better illustrate the effectiveness of our study, which is helpful in understanding some pharmacological properties of the compounds[15], DNA and RNA helix formation[16], and marine and environmental pollutants[17].

METHODS

The solubility assay of a salt with a model compound involves the preparation of a series of 10 sample salt stock solutions with concentration ranging from 0 to 2 molal. Each solubility experiment consisted of twelve tubes with 10 of them containing 5mL of salt stock solution and 2 of them containing 5 mL buffer. The buffer we use consists of 10mM K_2HPO_4 at pH=7.3. Then, excess model compound is added into each tube to saturate the solution and all solutions are incubated in water bath shaker at 298K for 10-14 days to achieve full saturation, where experimental $\mu_{23} = \Delta\mu_{23} = m$-value according to Equation 2-2 since initial μ_{23} is 0. Dilution

of the solutions is made after the incubation to guarantee readable absorbance for each sample measured by UV-Vis spectrophotometer. The peak absorbance, whose corresponding wavelengths are different for different model compounds, is used as the raw data. Molal solubility can be determined from Equation 5, where χ is a factor that converts molarity (mol/L) to molality (mol/Kg H_2O); A is the absorbance of each sample at its corresponding wavelength proportional to its molarity and A* is the average value of the absorbance of the two saturated nucleobase solutions with no salt in buffer at the same wavelength.

$$m_2^{ss}/ m_2^{*} = \chi A/ \chi A^* \qquad (5)$$

To determine the chemical potential derivative μ_{23}, $-\ln(m_2^{ss}/ m_2^{*})$ is plotted with the molal salt concentration m_3. For most model compounds these plots are linear and the slope is μ_{23}/RT, where R is ideal gas constant (1.987 cal $K^{-1}mol^{-1}$) and T is the room temperature (298 K). Where the plot is nonlinear, a quadratic fit is used and μ_{23} is determined from the initial slope. In general, a positive slope indicates an unfavorable interaction between salts and bases and a negative slope indicates a favorable interaction between salts and bases.

RESULTS

Salt-Model Compound Interaction Data

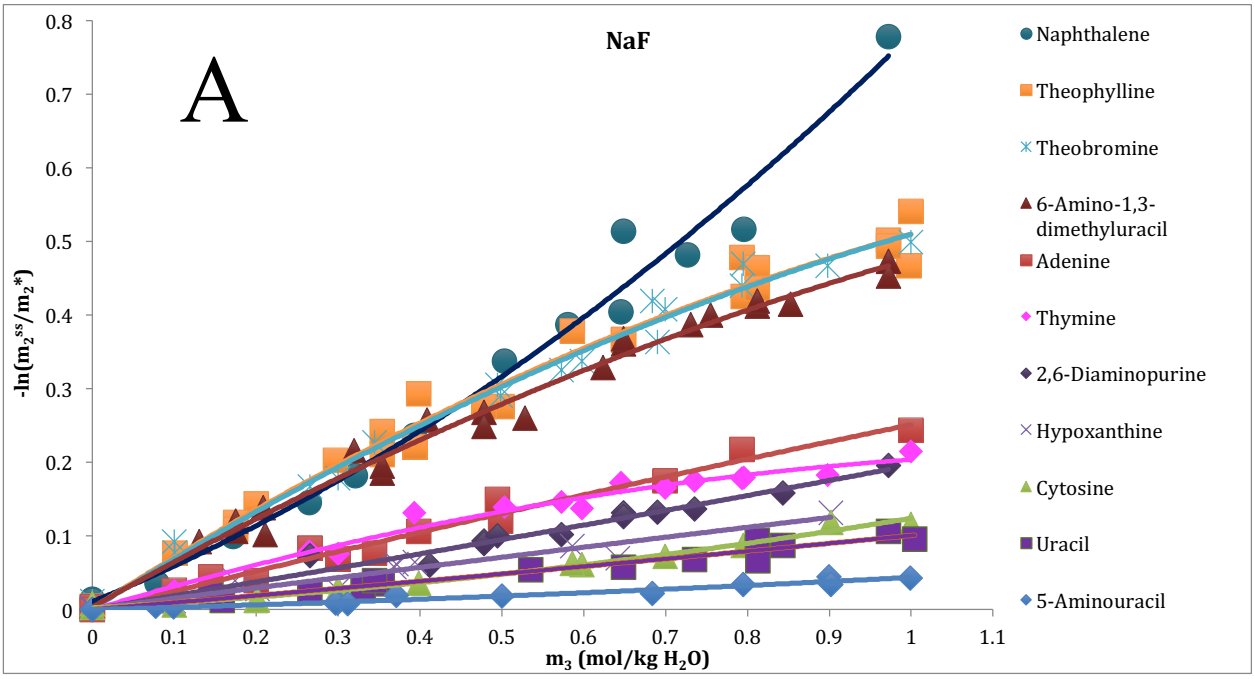

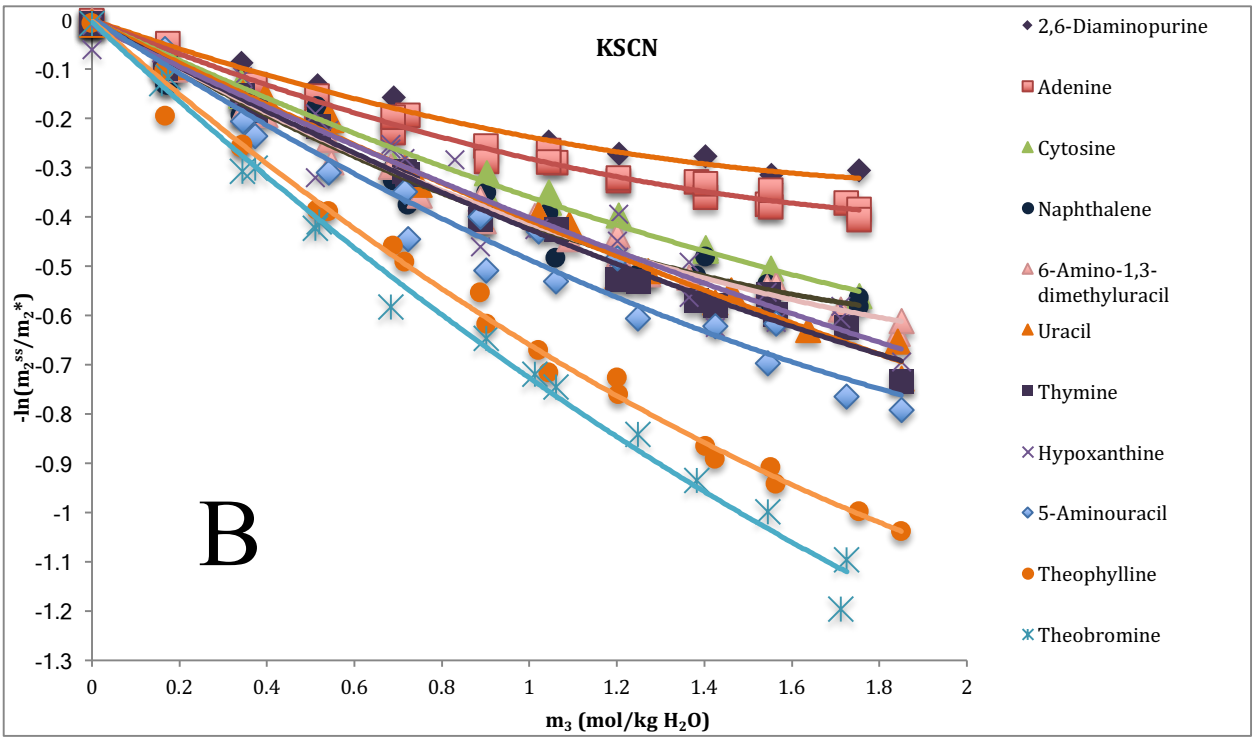

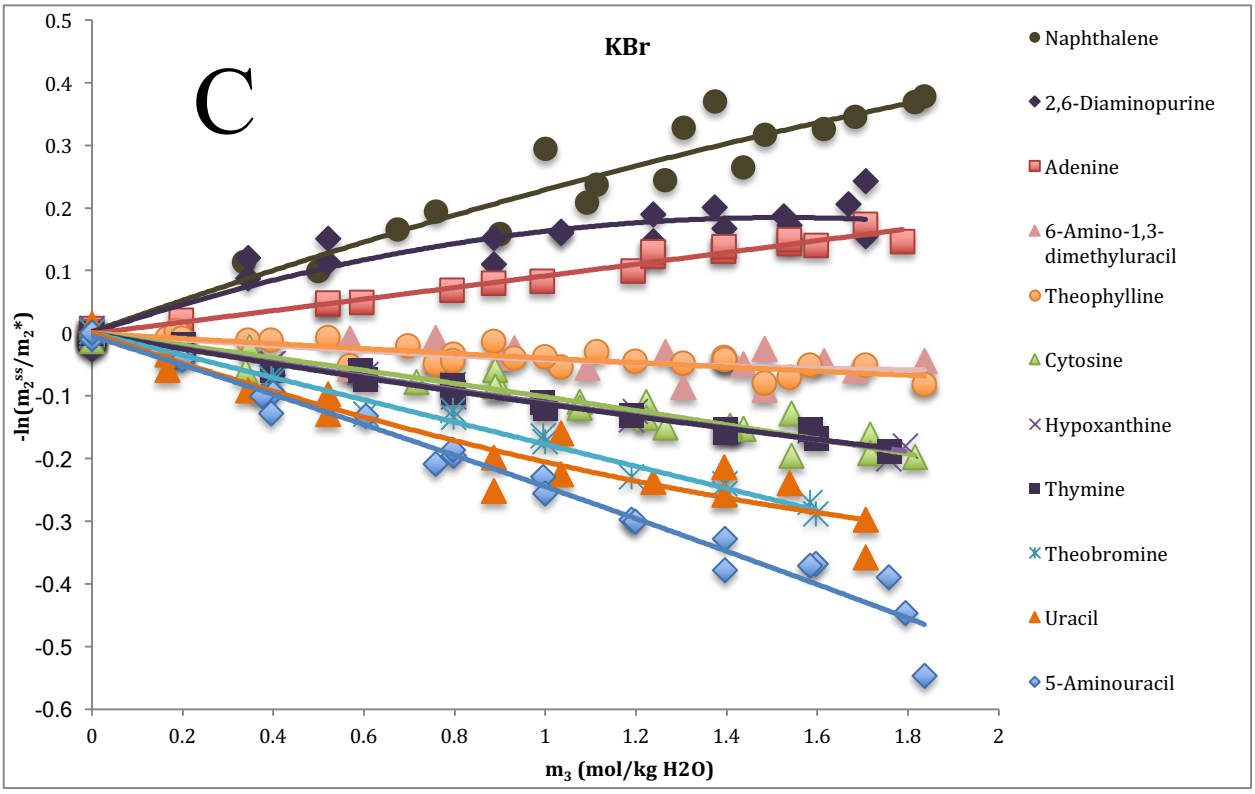
C
KBr
-ln(m2ss/m2*)
m3 (mol/kg H2O)
Naphthalene
2,6-Diaminopurine
Adenine
6-Amino-1,3-dimethyluracil
Theophylline
Cytosine
Hypoxanthine
Thymine
Theobromine
Uracil
5-Aminouracil

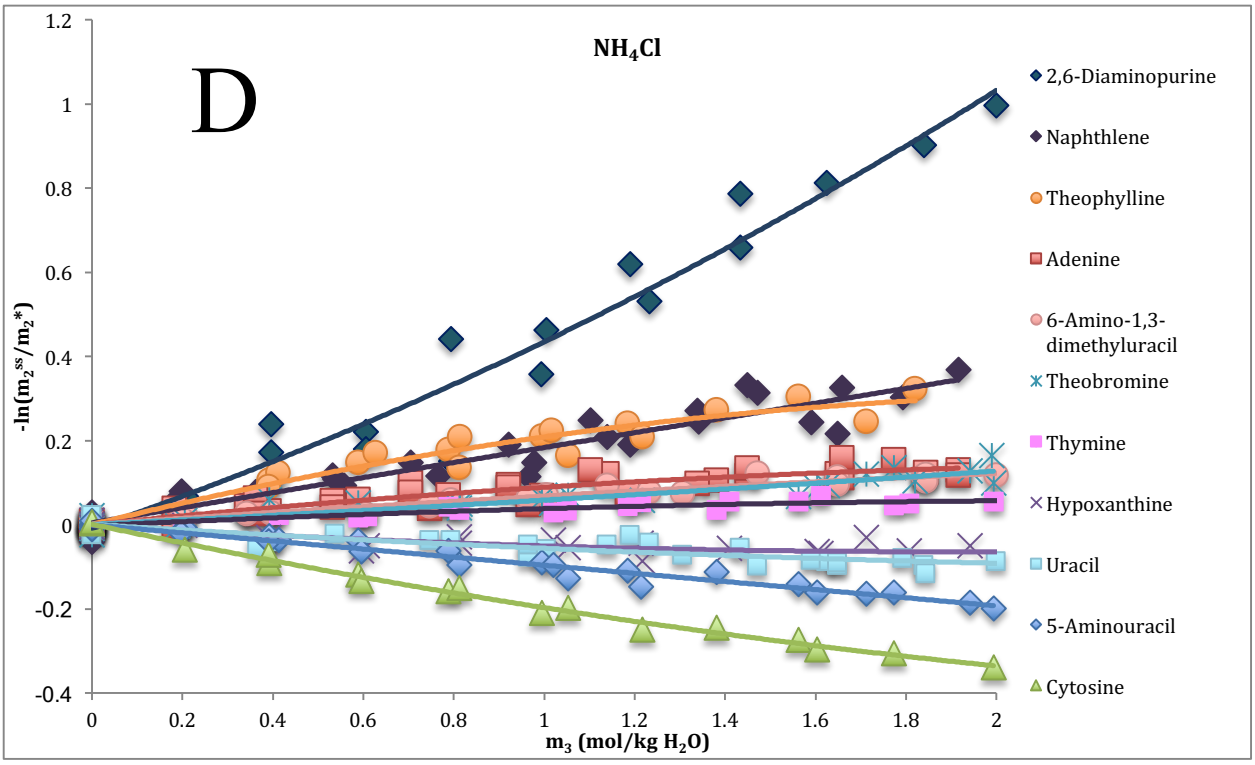
D
NH4Cl
-ln(m2ss/m2*)
m3 (mol/kg H2O)
2,6-Diaminopurine
Naphthlene
Theophylline
Adenine
6-Amino-1,3-dimethyluracil
Theobromine
Thymine
Hypoxanthine
Uracil
5-Aminouracil
Cytosine

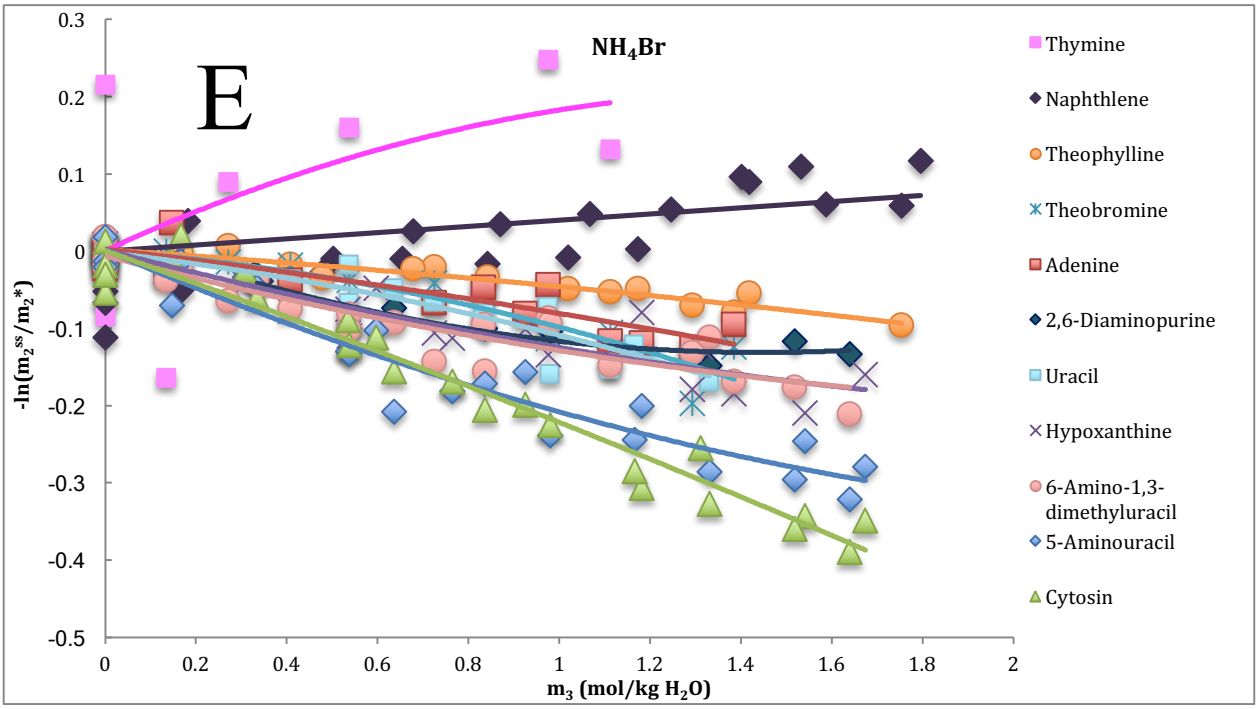

Figure 3. $-\ln(m_2^{ss}/ m_2^{*})$ vs. Salt molality

Figure 3 shows the $-\ln(m_2^{ss}/ m_2^{*})$ against the molality of the 5 different Hofmeister salts. By least square fitting forced the intercepts at zero, the slope of each curve equals to the μ_{23}/RT value of the corresponding model compound according to Equation 2. Table 1 lists the μ_{23} values of each pair of salt and model compound. Although some of the percentage errors of fitting are larger than the others, the absolute errors are consistent throughout these salt-base pairs. In general, salt-base interactions are independent of salt concentration by showing a linear regression curve during the low concentration range. However, the quadratic pattern is more obvious for some salt-base pairs, particularly the ones of thymine, when the salt concentrations increase. The line diagrams below in Figure 4 can better visualize and compare the unitless μ_{23}/RT values for further analysis and interpretation.

μ_{23} Data

Table 1. μ_{23} data of sodium fluoride and potassium bromide with 12 model compounds. Thymine (Thy), Hypoxanthine (Hyp), Theobromine (Tbr), Theophylline (Tpy), 5-Aminouracil (5AU), Adenine (Ade), 6-Amino-1, 3-dimethyluracil (6-DMU), Uracil (Ura), 2,6-Diaminopurine (2,6-DAP), Naphthalene (Nap), Cytosine (Cyt)

μ_{23} (cal mol^{-1} M^{-1})	NaF	KSCN	KBr	NH4Cl	NH4Br
Thymine	195 ± 12	-288 ± 34	-74.5 ± 4.1	29.1 ± 5.6	35.0 ± 12.8
Hypoxanthine	87.2 ± 5.5	-268 ± 9	-70.6 ± 4.9	-39.7 ± 10.2	-90.8 ± 21.9
Theobromine	415 ± 17	-495 ± 38	-105 ± 5	30.7 ± 13.0	-25.5 ± 39.1
Theophylline	424 ± 18	-459 ± 18	-25.9 ± 2.8	157 ± 19	-23.1 ± 9.9
5-Aminouracil	17.5 ± 3.7	-339 ± 18	-141 ± 11	-56.6 ± 7.5	-152 ± 26
Adenine	158 ± 10	-215 ± 15	53.2 ± 4.6	59.9 ± 11.2	-40.7 ± 28.1
6-Amino-1,3-dimethyluracil	381 ± 17	-302 ± 13	-34.0 ± 3.0	44.1 ± 7.8	-170 ± 21
Uracil	55.2 ± 9.2	-263 ± 25	-148 ± 13	-39.8 ± 11.5	-81.2 ± 20.1
2,6-Diaminopurine	109 ± 16	-183 ± 11	144 ± 25	210 ± 59	-97.4 ± 16.3
Naphthalene	294 ± 23	-314 ± 26	154 ± 14	107 ± 29	47.4 ± 22.3
Cytosine	61.7 ± 6.5	-248 ± 10	-56.1 ± 4.2	-133 ± 10	-123 ± 22

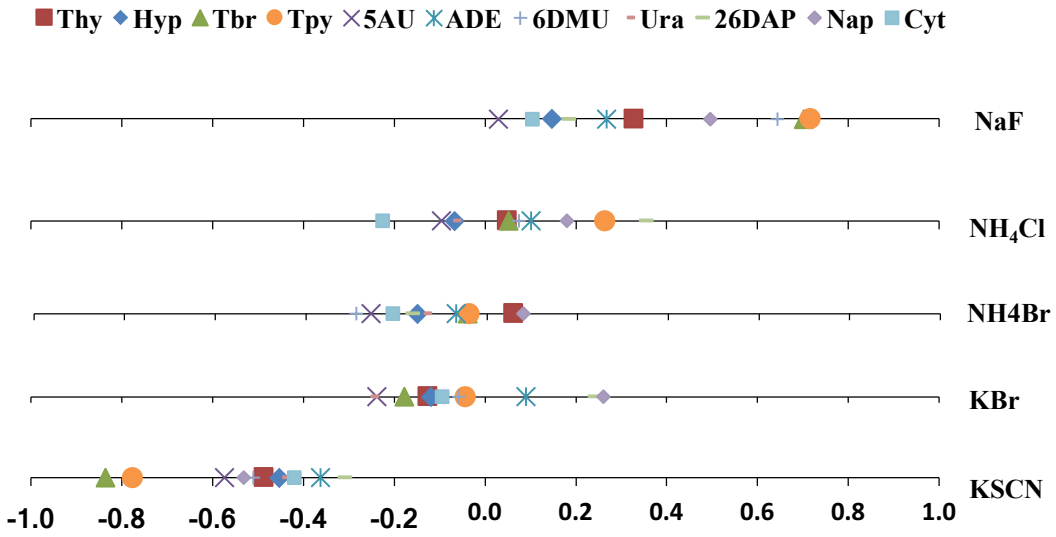

Figure 4. μ_{23}/RT for all bases and salts investigated in the solubility assay.

NaF interacts unfavorably with all aromatic compounds and nucleobases studied ($\mu_{23} > 0$) as expected because the Na^+ and F^- ions are tightly hydrated and prefer to interact with water than

with the hydrocarbon and polar groups of the bases. KSCN interacts favorably with all the model compounds studied since K^+ and SCN^- ions are less hydrated so that their interactions with model compounds are more likely. KBr, on the other hand, where the K+ and Br- ions are less tightly hydrated and so more likely to interact with the model compound, exhibits favorable interactions with the more polar of the set of nucleobases studied, and unfavorable interactions with naphthalene and the less polar nucleobases. Similar interpretations can also be applied to NH_4Cl and NH_4Br, where NH_4^+ is less hydrated than K^+ and Cl^- is slightly more hydrated than Br^-.

Comparison between different bases:

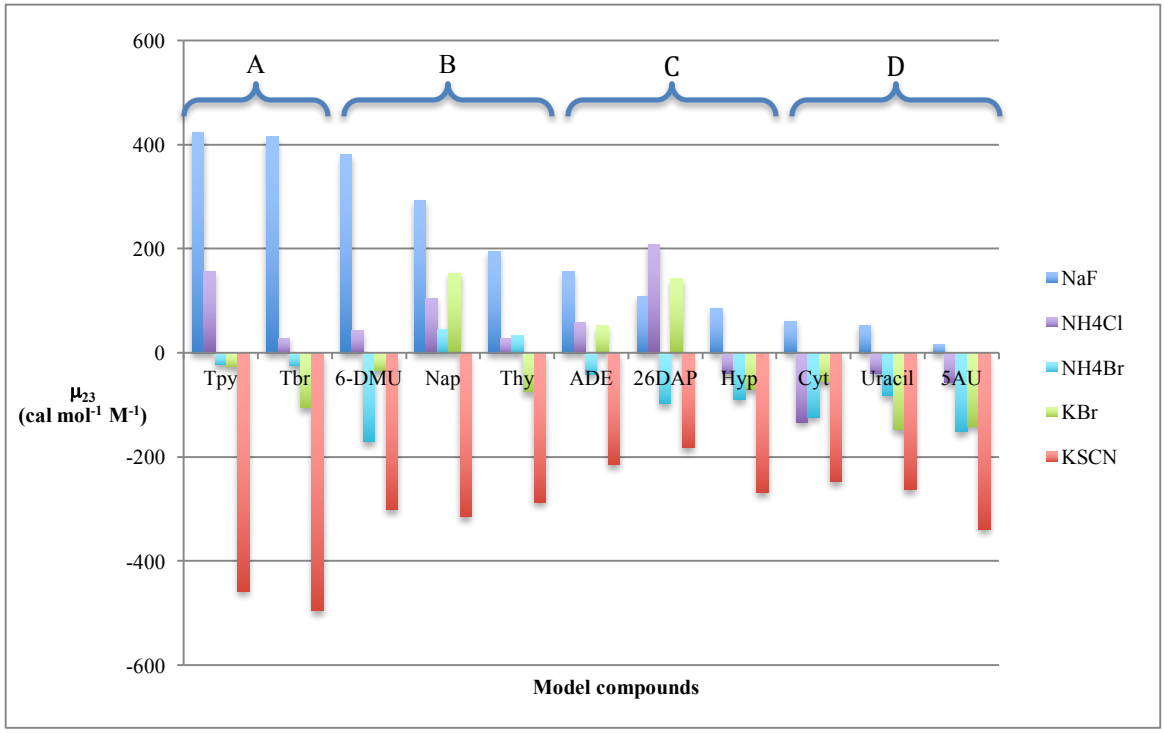

Figure 5. Comparison between interactions of different Hofmeister salts with the same base. (Using decreasing orders of μ_{23} of NaF to arrange the model compounds in the figure.)

The model compounds can be classified into 3 groups: Pyrimidine derivatives, Purine derivatives, Naphthalene. Interestingly, by ranking in decreasing orders of μ_{23} of NaF, the bases follow the order of (A) purine with methyl group (Tpy, Tbr), (B except Nap) pyrimidine with methyl group (6DMU, Thy), (C) purine without methyl group (Ade, 26DAP, Hyp), and lastly (D) pyrimidine without methyl group (Cyt, Ura, 5AU). In the following section, I will pick 2 pairs from pyrimidine group and 2 pairs from purine group to compare their interactions with different salts.

Ade vs Hyp

Ade and Hyp are two purine bases with only one functional group difference. The Sp3 N of the Ade is replaced by an carbonyl O. According to the ASA table in appendix, the major surface area differences between these two molecules are that Ade has an Sp3 N component of 79.2 A^2 whereas Hyp has 0 A^2; Hyp has a carbonyl O component of 44.7 A^2 whereas Ade has 0 A^2. In general, the interactions between Hyp and the 5 salts are more favorable than interactions between Ade and these salts based on the more negative μ_{23} values of Hyp. Ade and Hyp both show favorable interactions with KSCN and NH_4Br and unfavorable interactions with NaF. However, KBr and NH_4Cl interact favorably with Hyp whereas the interactions with Ade are unfavorable. These suggest that the five salts may interact with an carbonyl O surface more favorably than an Sp3 N surface.

Tbr vs Tpy

Tbr and Tpy are two purine bases with only a difference of a methyl group's position. This shift of the methyl group results in a slightly different surface areas. According to ASA table in appendix, Tbr has larger aliphatic C and carbonyl O surface areas but smaller aromatic C and N surface areas than Tpy. Because of their structural similarity, they both show favorable interactions with KBr, KSCN, and NH_4Br while unfavorable interactions with NaF and NH_4Cl. However, the slight difference in surface areas also makes the interactions of Tbr with KBr, KSCN, NaF and NH_4Cl more favorable than those of Tpy.

Thy vs 5AU

Thy and 5AU are two pyrimidine nucleobases that differ by one functional group. An amino group in 5AU replaces the methyl group of the Thy. According to the table in the appendix, the surface area for aliphatic C is 81.5 A^2 on Thy compared to 0 A^2 on 5AU; whereas the surface area for Sp3 N is 0 A^2 on Thy compared to 59.7 A^2 on 5AU. In general, the interactions between 5AU and the 5 salts are more favorable than interactions between Thy and these salts based on the more negative μ_{23} values of 5AU. The interactions of KBr and NH_4Cl with 5AU are favorable whereas those with Thy are unfavorable. These suggest that these 5 salts may favor Sp3 N surface more than aliphatic C surface.

Thy vs Ura

Ura is another pyrimidine nucleobase that differs with Thy by removing the methyl group of the thymine. According to the table in appendix, the component of aromatic C surface area in Thy is 43.1 A^2 and in Ura is 115 A^2. The aliphatic C component of surface area of Thy 81.5 A^2 whereas 0A^2 in Ura. In general, the interactions between uracil and the 5 salts are more favorable than interactions between Thy and these salts based on the more negative μ_{23} values of Ura. The interactions of NH_4Cl and NH_4Br with Ura are favorable whereas those with Thy are unfavorable. These suggest that these 5 salts may favor aromatic C surface more than aliphatic C surface.

Comparison between different salt series

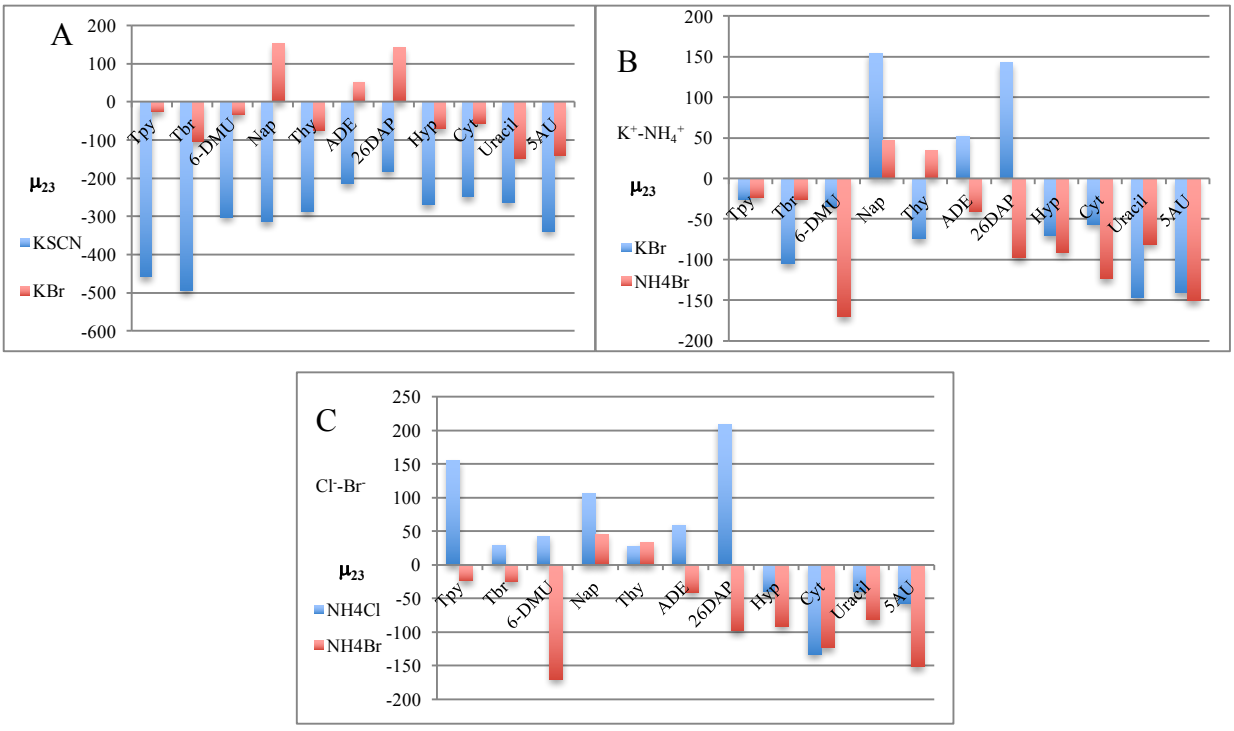

Figure 6. μ_{23} for KBr and KSCN and all bases investigated (A); μ_{23} for KBr and NH_4Br and all bases investigated (B); μ_{23} NH_4Cl and NH_4Br and all bases investigated (C).

Here, we compare the differences of preferential interactions between Br^- and SCN^-, K^+ and NH_4^+, and Cl^- and Br^-. We keep the cation the same to compare the anions' preferential interactions and keep the anion the same in order to compare the cations' preferential interactions. The results are then compared with Hofmeister Series in Figure 1.

Br^- and SCN^-

KSCN has favorable interactions with all the bases with negative μ_{23} values. KBr, however, shows unfavorable interactions with Ade, Nap, and 26DAP. Considering the μ_{23} values of those bases favorably interact with KBr, the magnitudes are smaller than those with KSCN. These suggest that SCN^- interacts more favorably with model compounds than Br^-. The result matches with the Hofmeister Series and verifies that SCN^- has a more destabilizing effect on biopolymer processes than Br^-.

K^+ and NH_4^+

KBr has favorable interactions with most of the bases with negative μ_{23} values except Ade, Nap, and 26DAP. NH_4Br also shows favorable interactions with most of the bases except Nap and Thy. Considering the μ_{23} values of those bases, the magnitudes of the ones with NH_4Br are slightly larger than those with KBr. These suggest that NH_4^+ interacts more favorably with model compounds than K^+. The result matches with the Hofmeister Series and verifies that K^+ has a more stabilizing effect on biopolymer processes than NH_4^+.

Cl^- and Br^-

NH_4Cl in general shows unfavorable interactions with most of these bases except Hyp, 5AU, Ura, and Cyt. NH_4Br, on the other hand, interact favorably with most of these model compounds except Nap and Thy. These suggest that Br^- interacts more favorably with model compounds than Cl^-. The result matches with the Hofmeister Series and verifies that Cl^- has a more stabilizing effect on biopolymer processes than Br^-.

DISCUSSION

Interaction Potentials

According to Eq. 3 the interaction potential value (α_i) was calculated to quantify the interactions between each salt and each functional group *i* (Aromatic C, Aromatic N, Aliphatic C, Carbonyl O, Sp3N). The α_i values are listed in Table 2 with their uncertainties.

Table 2. Interaction potentials α_i for each salt (unit is cal mol^{-1} m^{-1} A^{-2}).

α_i values	NaF	KSCN	KBr	NH4Cl	NH4Br
Aromatic C	1.07 ± 0.0778	-1.09 ± 0.0926	0.534 ± 0.0481	0.345 ± 0.101	0.132 ± 0.0788
Aromatic N	0.249 ± 0.0825	-0.969 ± 0.105	-0.171 ± 0.0428	0.233 ± 0.0918	0.116 ± 0.154
Aliphatic C	2.66 ± 0.0695	-1.43 ± 0.127	0.405 ± 0.0407	1.00 ± 0.0664	0.227 ± 0.123
Carbonyl O	-0.817 ± 0.798	-1.41 ± 0.173	-2.02 ± 0.0910	-1.47 ± 0.128	-1.11 ± 0.184
Sp3N	0.259 ± 0.0797	-0.248 ± 0.0886	0.631 ± 0.0973	0.515 ± 0.233	-0.934 ± 0.126

α_i values for each type of surface area are categorized into the 5 Hofmeister salts that we are studying in Figure 7.

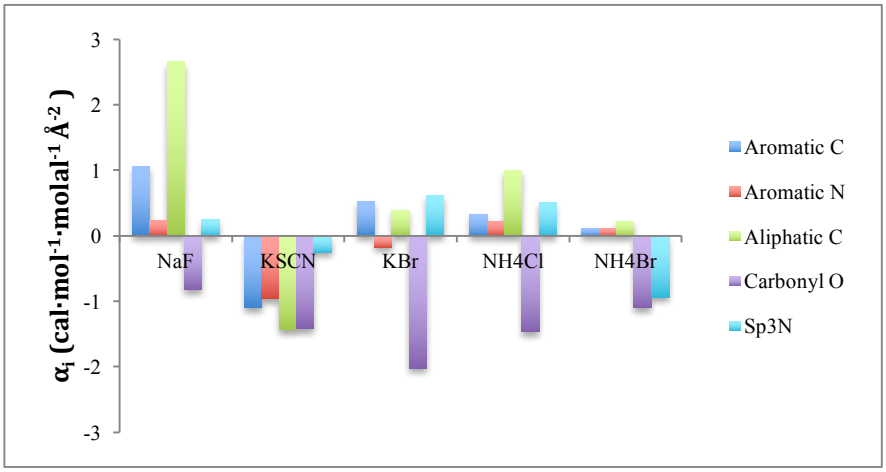

Figure 7. Breakdown of surface interaction potentials α_i by salts.

We also plotted the α_i values for each type of surface area using a bar graph with error bars to compare the salt-base surface interactions in Figure 8.

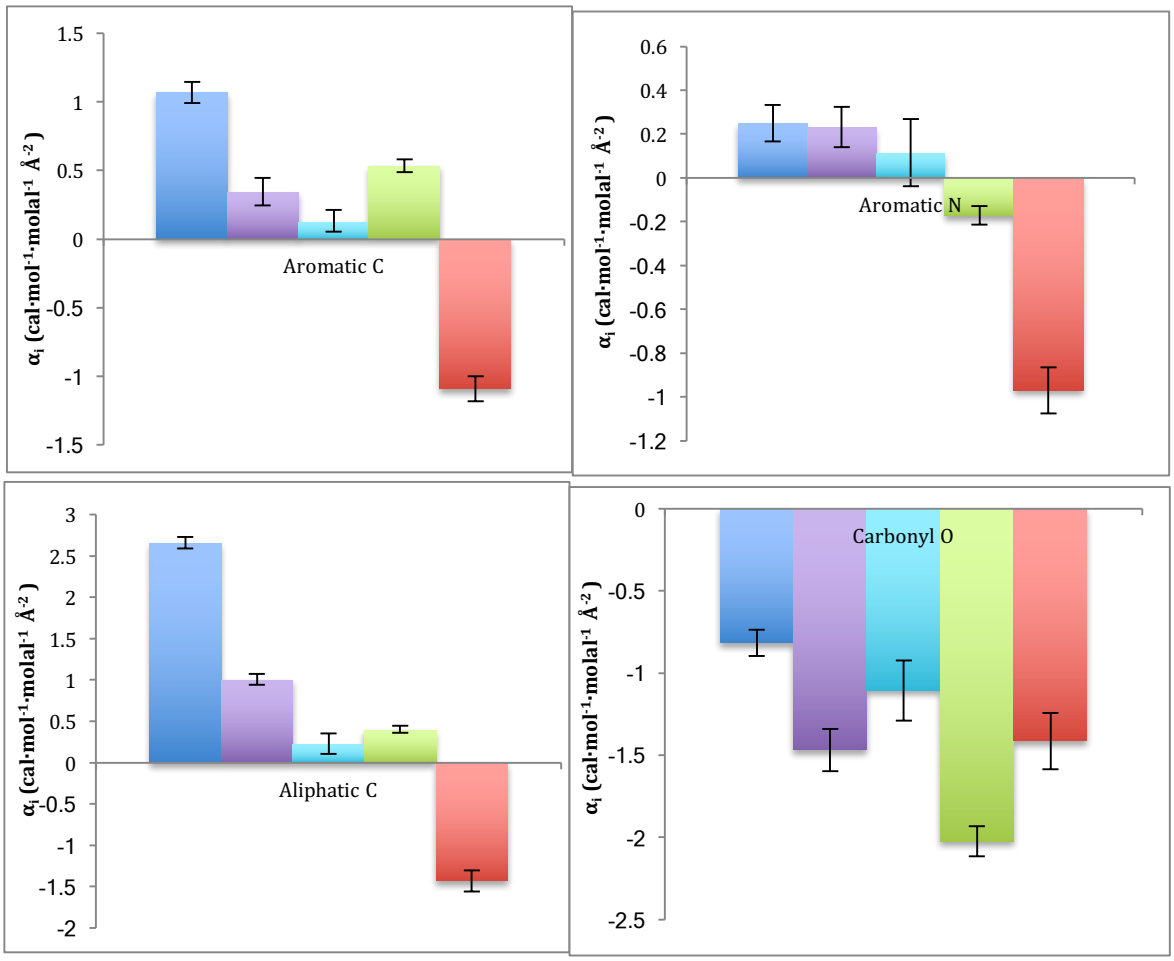

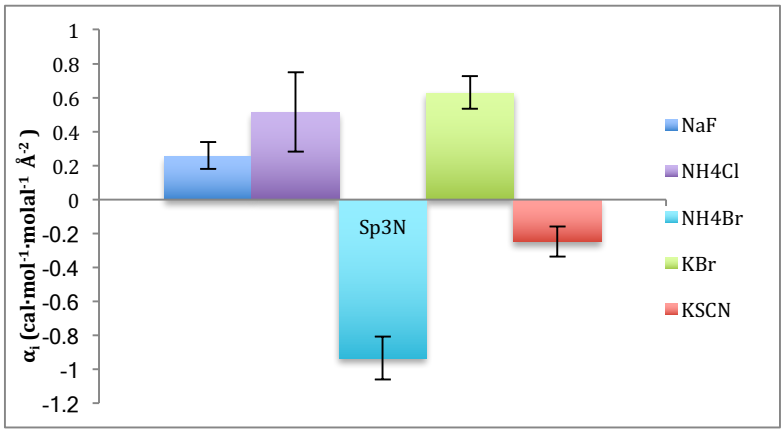

Figure 8. Breakdown of surface interaction potentials α_i by surface type i. If $\alpha_i > 0$, the neutral salt is excluded; $\alpha_i < 0$, the neutral salt is accumulated; if α_i is close to 0, the neutral salt is neither accumulated nor excluded from the base surface.

KSCN has all negative α_i values, showing favorable interactions with all these 5 surface types, which corresponds to the results that it has the strongest favorable interactions with all the model compounds. NaF has a large positive α_i value for aliphatic C, indicating unfavorable interactions with the aliphatic C surfaces, which corresponds to the results that it has higher μ_{23} values for model compounds rich in aliphatic C surfaces like Tbr, Tpy, and 6DMU.

α_i values of aromatic C and aromatic N are distinctively different for all 5 salts studied. This contradicts to the assumption of previous studies that combine aromatic C and aromatic N as the same group called "ring". It provides evidence for future studies to treat aromatic C and aromatic N surfaces separately. Overall, aromatic N has smaller interaction potentials than aromatic C.

For aliphatic C, the calculated α_i values demonstrate favorable interaction with KSCN and unfavorable interactions to the rest salts. The calculated α_i values of Sp3 N show that NH_4Br is extremely larger in magnitude, indicating its very favorable interaction with this surface type. By comparing α_i values, the unfavorability of NH_4Cl is less than that of NaF with aliphatic C

whereas the unfavorability of NH_4Cl is more than that of NaF with Sp3 N; NH_4Br has unfavorable interaction with aliphatic C, but favorable interaction with Sp3 N. The interactions between salts and carbonyl O surface are all favorable. KBr has the strongest favorable interactions ($\alpha_{\text{aliphatic C}} = -2.21$ cal $mol^{-1}m^{-1}A^{-2}$) and NaF has the weakest favorable interactions ($\alpha_{\text{aliphatic C}} = -1.06$ cal $mol^{-1}m^{-1}A^{-2}$).

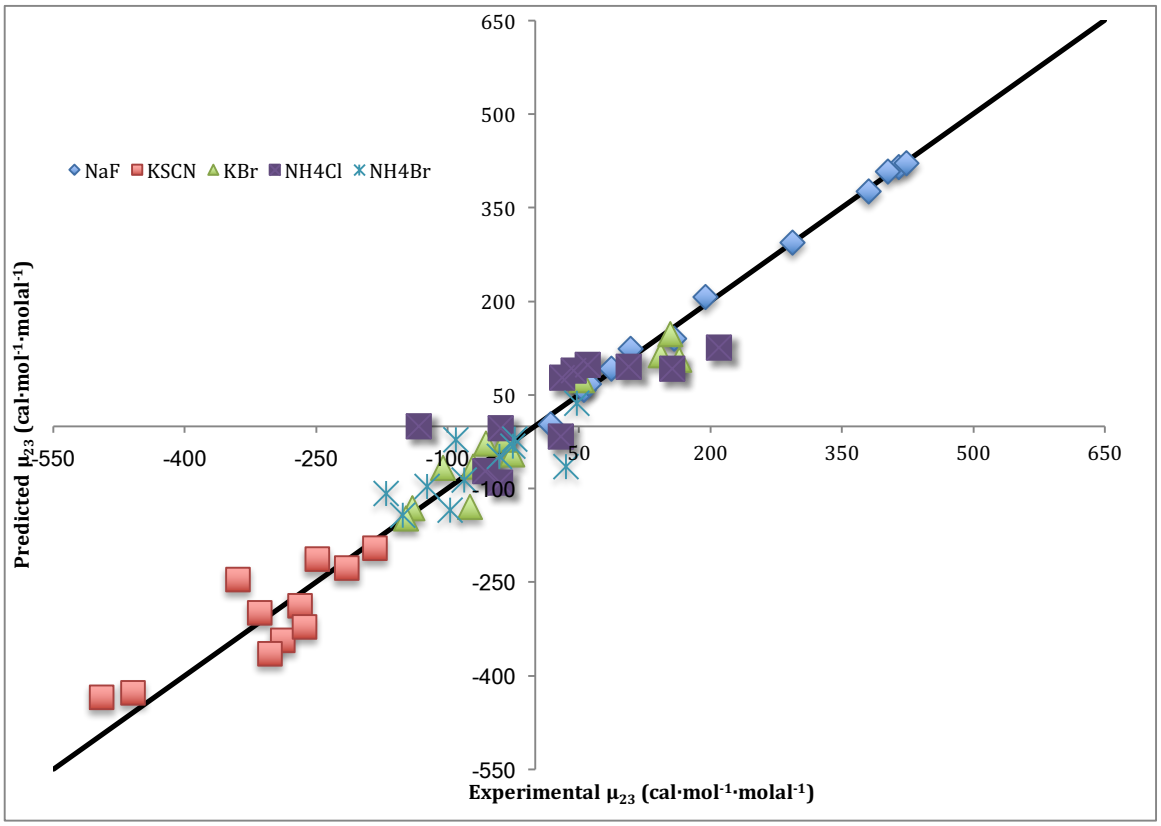

Figure 10. Predicted μ_{23} vs. observed μ_{23}.
The equation of the black line is $\mu_{23,\text{ predicted}} = \mu_{23,\text{ experimental}}$.

The predicted μ_{23} values were back calculated from α_i values and the ASAs of each surface type by using Equation 3. Predicted values are listed in Table 2 in appendix. We plotted the predicted μ_{23} values against observed μ_{23} values in Figure 10 and the values are generally around the $\mu_{23,\text{ predicted}} = \mu_{23,\text{ experimental}}$ line. The outliers on this plot have been experimentally tested for at

least 3 times to eliminate the deviations due to random errors.

Relative Strengths of Preferential Interactions of Salt Ions

In order to determine the interaction potentials of each salt ion, we have to compare the α value to a reference ion set as 0. In this study, we propose to use Sodium ion (Na^+) as the reference ion and aromatic C and aliphatic C can be studied based on this assumption. With the α value one of the ion is known for a certain type of surface, the α value of the other ion of the salt can be obtained by subtracting the known alpha value from the total α value of the salt (in Table 2). To cover all ions, we studied by this method, we cited our lab's previously quantified NaSCN preferential interactions data (Cheng et. al., in preparation). Figure 11 shows the relative preferential interactions of 7 ions with the 2 surface types.

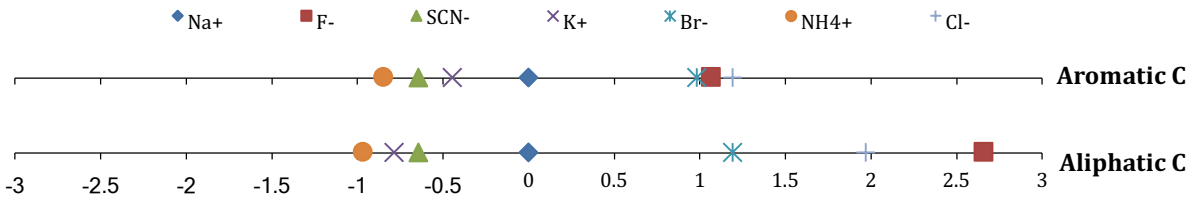

Figure 11. The relative alpha value of each salt-base surface type interaction using Na^+ ion as reference (unit is cal mol^{-1} m^{-1} A^{-2}).

The aliphatic C surface shows the wider range of 3.62 cal mol^{-1} m^{-1} A^{-2}, while the aromatic N surface shows the narrower range of 2.04 cal mol^{-1} m^{-1} A^{-2}. The alpha values of aliphatic C show an anion favorability trend of $SCN^- < Br^- < Cl^- < F^-$ and a cation trend of $NH4^+ < K^+ < Na^+$, both of which perfectly match the Hoffmeister series (Figure 1). Similarly, for aromatic C, it generally follows the Hofmeister Series for both anions and cations. Additional studies are

required to make ion separation of other surface types possible.

Accumulation and Exclusion of Hofmeister Salts and Ions

According to the Equation 4-2 and 4-3, we are able to calculate K_p values for Hofmeister salts with different surface types listed in Table 3. When $K_p = 1$, no accumulation or exclusion of salt ions. If $K_p > 1$, accumulation of salt occurs; if $K_p < 1$, exclusion of salt occurs.

Table 3. Kp values of salts with different surface types.

K_p values	NaF	KSCN	KBr	NH_4Cl	NH_4Br
Aromatic C	0.68 ± 0.02	1.29 ± 0.02	0.85 ± 0.01	0.90 ± 0.03	0.96 ± 0.03
Aromatic N	0.93 ± 0.02	1.26 ± 0.03	1.05 ± 0.01	0.93 ± 0.03	0.96 ± 0.05
Aliphatic C	0.20 ± 0.02	1.38 ± 0.03	0.88 ± 0.01	0.71 ± 0.02	0.93 ± 0.04
Carbonyl O	1.24 ± 0.02	1.37 ± 0.05	1.59 ± 0.03	1.43 ± 0.04	1.35 ± 0.06
Sp3N	0.92 ± 0.02	1.07 ± 0.02	0.82 ± 0.03	0.85 ± 0.07	1.30 ± 0.04

According to Table 3, KSCN is accumulated at all surfaces whereas NaF and NH_4Cl are only accumulated at carbonyl O surface. NH_4Cl and NH_4Br have similar effects for all surface types except Sp3N, where NH_4Br has a strong accumulation effect while NH_4Cl is excluded. This matches the preferential interaction data that Br^- has a stronger favorable interaction with Sp3 N than Cl^-. Aromatic and aliphatic C surfaces show exclusion effect to all salts except KSCN. In addition, all salts are accumulating to carbonyl O surface. Generating heat maps of model compounds is a better way to explicitly demonstrate the exclusion and accumulation effects. Here, we pick 6DMU, which has all 5 surface types, as an example.

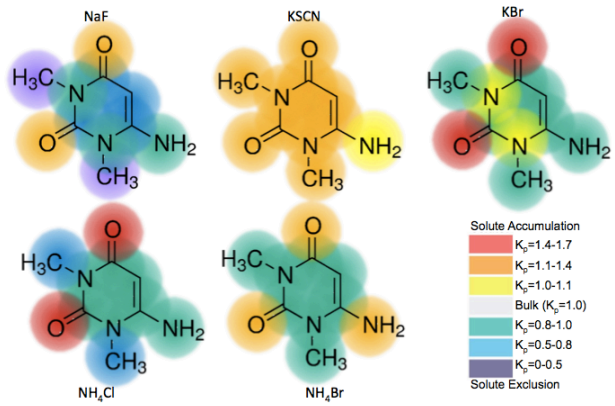

Figure 12. K_p value heat map of 6DMU.

According to Figure 12, we can visualize the general accumulation effect of KSCN and exclusion effect of NaF based on the brightness of the color of the molecule and are able to predict that KSCN has generally favorable interactions with 6DMU while NaF has unfavorable interations.

Using similar separation method for preferential interactions and Equation 4-3, K_p values of ions can also be deduced. Here, we assigned $K_{p,\ Na^+}$ to be 0 as reference point[14] and used NaSCN data from previous studies. Based on this assumption, we can quantify K_p values of different ions with aromatic C and aliphatic C. We also tried to use $K_{p,\ K^+}$ to be 0 as reference point only for aliphatic C surface to obtain reasonable K_p values for all ions. The K_p values at aromatic C and aliphatic C surfaces are listed in Table 4.

Table 4. K_p value of ions at aromatic C and aliphatic C surfaces.

K_p	Na^+	F^-	SCN^-	K^+	Br^-	$NH4^+$	Cl^-
Aromatic C	0.00	1.36 ± 0.05	2.35 ± 0.06	0.23 ± 0.11	1.47 ± 0.14	0.45 ± 0.19	1.35 ± 0.25
Aliphatic C (Na^+ as reference)	0.00	0.41 ± 0.04	2.87 ± 0.05	-0.12 ± 0.12	1.88 ± 0.14	-0.03 ± 0.22	1.44 ± 0.26
Aliphatic C (K^+ as reference)	0.12 ± 0.12	0.29 ± 0.16	2.76 ± 0.07	0.00	1.77 ± 0.02	0.09 ± 0.10	1.32 ± 0.14

The Kp values of ions we got is generally comparable to the published data[13]. Based on Table 4, cations are strongly excluded by both aromatic and aliphatic C surfaces, while SCN^- is strongly accumulated. The order of K_p values of anions follows the Hofmeister series whereas cations have some deviations. Most ions behave similarly for both aromatic and aliphatic C surfaces except F^-, which accumulates at aromatic C surfaces and excluded by aliphatic C surfaces. Setting K^+ as reference point of aliphatic C surface gives similar results for all ions as using Na^+ as reference point. This also verifies that K^+ and Na^+ rank very similar in Hofmeister series. Additional studies are required to make ion separation of other surface types possible.

Comparison with literature data

To evaluate the effectiveness of our prediction and illustrate the usefulness of this study, we predicted μ_{23} values of many other compounds based on Equation 3 and they are compared with experimental μ_{23} from published literature about pharmaceutical, environmental, and biological sciences[15-17]. These totally 24 experimental data points include the μ_{23} between the 5 salts we studied with purine, pyrimidine, and aromatic compounds, most of which are not used as our model compounds (eg. xylene, benzene, and toluene).

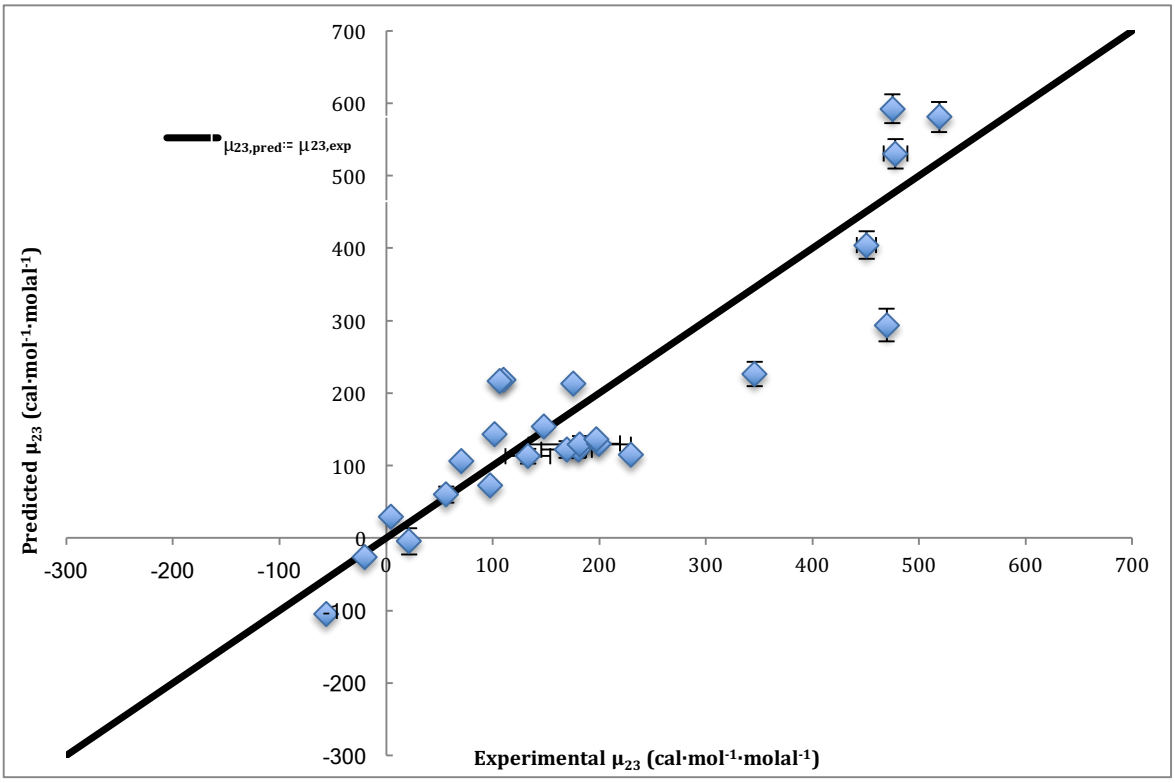

Figure 13. Predicted μ_{23} vs. experimental μ_{23} from literature.

In general, our predicted μ_{23} values matches with most of the experimental μ_{23} values according to Figure 13. The literature data and predicted values are listed in Table 3 in appendix. Our predicted values are more accurate for smaller interactions than for larger interactions and data points with relative large discrepancies to the predicted values are from benzene and xylenes. Further studies are needed to refine our predicting parameters, namely alpha values.

CONCLUSION

The interactions between Hofmeister salts and nucleobases and aromatic compound vary significantly between favorable and unfavorable interactions. Salt has the ability to either increase or decrease the solubility of the bases, which can be explained by their differences in

interacting with various surface types of the bases, namely aromatic C, aromatic N, aliphatic C, carbonyl O, and Sp3 N. Results of this study indicates that for all the eleven bases investigated in this study, KSCN has the most favorable interactions whereas NaF has the most unfavorable interactions except with 26DAP. The differences in their ability to decrease (unfavorable interaction) or increase (favorable interaction) the solubilities of bases corresponds with their rank orders among the Hofmeister series, in which the Na^+ and F^- are at the stabilizing end but SCN^- ion is at the destabilizing end.

Through one-way analysis, the breakdown of nucleobase's surface types allows us to study the specific interactions between salts and biopolymer surfaces. Here, the interactions between different salts with aromatic carbon and aromatic nitrogen surfaces show distinct interaction potentials, α_i values, which indicates previous consumption of combine aromatic carbon and aromatic nitrogen into same group is inappropriate. Setting Na^+ as a reference point, relative strength of interaction potentials of Hofmeister ions with aromatic and aliphatic C surfaces are obtained, which in general follows the Hofmeister series.

The quantities describing accumulation and exclusion of Hofmeister salts, K_p, are also obtained through calculation. Using Na^+ as a reference, a dissection of salts' K_p values to get ions' K_p values illustrates that aromatic and aliphatic C surface accumulates SCN^- strongly and strongly excludes cations. The K_p values we got are comparable to published data. Further studies are required to make dissections of other surfaces possible.

The quantified α_i values and ASA data are used to predict μ_{23} values. These predictions are

compared with both our experimental data and published experimental data. The results confirm the effectiveness of our method and indicate potential applications in pharmaceutical, environmental, and biological studies. Yet, method refinements and data collections are still needed to make these applications possible.

REFERENCES

1. Pegram, L. M., et al. 2010. Why Hofmeister effects of many salts favor protein folding but not DNA helix formation. Proc. Natl. Acad. Sci. U. S. A. **107:**7716-7721. doi: 10.1073/pnas.0913376107.
2. Hofmeister, F., 1888. On the understanding of the effects of salts. Arch Exp Pathol pharmakol. **24:**247-260.
3. Baldwin, R.L. 1996. How Hofmeister ion interactions affect protein stability. Biophys. J. **71:**2056-2063. doi: 10.1016/S0006-3495(96)79404-3.
4. Pegram, L.M. and Record, M.T.. 2007. Hofmeister salt effects on surface tension arise from partitioning of anions and cations between bulk water and air-water interface. Journal of Physical Chemistry. **112**(31):5411-5417.
5. Ray, A., and Nemethy, G.. 1971. Effects of ionic protein denaturants on micelle formation by nonionic detergents. J. Am. Chem. Soc. **93:**6787-6793. doi: 10.1021/ja00754a014.
6. Zhang, Y., and Cremer, P. S.. 2006. Interactions between macromolecules and ions: the Hofmeister series. Curr. Opin. Chem. Biol. **10:**658-663. doi: 10.1016/j.cbpa.2006.09.020.
7. Courtenay, E. S., Capp, M. W. and Record, M. T. 2001, Thermodynamics of interactions of urea and guanidinium salts with protein surface: Relationship between solute effects on protein processes and changes in water-accessible surface area. Protein Science, **10:** 2485–2497. doi:10.1110/ps.ps.20801
8. Knowles, D. B., et al., 2011, Separation of preferential interaction and excluded volume effects on DNA duplex and hairpin stability. Proceedings of the National Academy of Sciences, **108:** 12699-12704.
9. Record, M.T., Guinn, E., Pegram, L. and Capp, M., 2013. Introductory lecture: interpreting and predicting Hofmeister salt ion and solute effects on biopolymer and model processes using the solute partitioning model. Faraday discussions, **160:**9-44.
10. Nandi, P.K. and Robinson, D. R.. 1972. The effects of salts on the free energy of the peptide group. J. Am. Chem. Soc. **94**:1299-1308.
11. Pegram, L.M., and Record Jr, M. T.. 2008. Thermodynamic Origin of Hofmeister Ion Effects. J. Phys. Chem. B. 9428. doi: 10.1021/jp800816a.
12. Tsodikov, O.V., Record, M. T. Jr. and Sergeev, Y, V.. 2002. Novel computer program for fast exact calculation of accessible and molecular surface areas and average surface curvature. J. Comput. Chem. 23: 600-609. doi: 10.1002/jcc.10061.
13. Pegram, L. M., and Record, M. T. Jr. 2008. Quantifying accumulation or exclusion of H^+, HO^-, and Hofmeister salt ions near interfaces. Chemical Physics Letters. **467:**1-8. doi: 10.1016/j.cplett.2008.10.090.
14. Pegram, L.M., and Record, M. T. Jr., 2008. Hofmeister salt effects on surface tension arise from partitioning of anions and cations between bulk water and the air-water interface. J. Phys. Chem. B. **111:**5411-5417.

15. Perez-Tejeda, P., Maestre, A., Balon, M., Hidalgo, J., Munoz, M.A., and Sanchez, M., 1987. Setschenow Coefficients for Caffeine, Theophylline and Theobromine in Aqueous Electrolyte Solutions. J. Chem. Soc., Faraday Trans. **83:** 1029-1042.

16. Robinson, D. R., and Grant, M. E., 1966. The Effect of Aqueous Salt Solutions on the Activity Coefficients of Purine and Pyrimidine Bases and Their Relation to the Denaturation of Deoxyribonucleic Acid by salts. J Biol. Chem. **241:** 4030-4040.

17. Xie, W., Shiu, W., and Mackay, D., 1997. A Review of the Effect of Salts on the Solubility of Organic Compounds in Seawater. Marine Envir. Res. **44:** 429-477.

APPENDIX

Table 1. Contributions to water accessible surface area (ASA) (Å^2) from five different functional groups of aromatic compounds.

	Aromatic C	Aromatic N	Aliphatic C	Carbonyl O	Sp3 N
Thymine	43.1	60.0	81.5	86.8	0
Hypoxanthine	89.9	132	0	44.7	0
Theobromine	53.9	59.0	151	72.6	0
Theophylline	60.4	64.2	147	62.7	0
5-Aminouracil	42.6	60.0	0	89.7	59.7
6-Amino-1,3-dimethyluracil	37.7	5.26	141	70.9	71.9
Uracil	115	59.3	0	98.5	0
2,6-Diaminopurine	51.8	102	0	0	163
Naphthalene	275	0	0	0	0
Cytosine	71.4	53.9	0	47.8	63.7
Adenine	83.5	121	0	0	79.2

Table 2. Predicted μ_{23} calculated using Equation 3. (unit: cal·mol^{-1}·molal^{-1})

μ_{23}	NaF	KSCN	KBr	NH_4Cl	NH_4Br
Thymine	207±21	-344±36	-130±16	-16.8±26.4	-64.9±38.6
Hypoxanthine	92.4±21.4	-289±30	-64.9±14.0	-3.9±27.0	-22.3±35.6
Theobromine	415±25	-435±43	-67.0±17.9	77.5±30.2	-32.1±45.3
Theophylline	421±25	-428±42	-45.9±17.4	91.8±29.8	-20.5±44.4
5-Aminouracil	2.70±20.20	-246±31	-131±19	-72.3±35.2	-143±37
Adenine	140±23	-228±28	74.0±16.9	97.7±39.4	-49.0±40.5
6-Amino-1,3-dimethyluracil	376±25	-366±41	-21.8±21.2	88.4±29.7	-108±22
Uracil	57.8±21.7	-323±34	-148±17	-91.0±52.7	-86.9±30.8
2,6-Diaminopurine	123±26	-196±30	114±23	126±28	-134±31
Naphthalene	294±21	-300±26	147±13	94.8±33.1	36.4±30.8
Cytosine	67.2±18.9	-214±26	-27.6±16.3	-0.200±38.0	-96.8±31.3

Table 3. Literature μ_{23} and predicted $\mu_{23.}$ (unit: cal·mol^{-1}·molal^{-1})

Compound	Salt	Literature μ_{23}	Predicted μ_{23}
Caffeine[15]	KBr	21.4 ± 9.6	-4.57 ± 18.24
Theophylline[15]	KBr	-19.9 ± 0	-25.9 ± 2.8
Theobromine[15]	KBr	-56.1 ± 10.9	-105 ± 5
Thymine[16]	NH4Cl	4.70 ± 0	29.1 ± 5.6
Adenine[16]	NH4Cl	56.1 ± 0	59.9 ± 11.2
Benzene[17]	NaF	346 ± 3	226 ± 16
Toluene[17]	NaF	451 ± 0	404 ± 19
o-Xylene[17]	NaF	478 ± 0	530 ± 20
m-Xylene[17]	NaF	519 ± 0	581 ± 21
p-Xylene[17]	NaF	475 ± 0	592 ± 20
Naphthalene[17]	NaF	470 ± 0	294 ± 23
Benzene[17]	KBr	133 ± 15	113 ± 10
Toluene[17]	KBr	169 ± 11	122 ± 11
o-Xylene[17]	KBr	182 ± 0	129 ± 12
m-Xylene[17]	KBr	200 ± 0	130 ± 12
p-Xylene[17]	KBr	197 ± 0	136 ± 13
Naphthalene[17]	KBr	148 ± 0	154 ± 14
Benzene[17]	NH4Cl	97.7 ± 8.4	73.0 ± 21.4
Toluene[17]	NH4Cl	102 ± 52	143 ± 22
o-Xylene[17]	NH4Cl	110 ± 0	219 ± 22
m-Xylene[17]	NH4Cl	176 ± 0	213 ± 17
p-Xylene[17]	NH4Cl	106 ± 0	216 ± 24
Naphthalene[17]	NH4Cl	70.3 ± 0	107 ± 29
Phenanthene[17]	NH4Cl	230 ± 0	115 ± 34

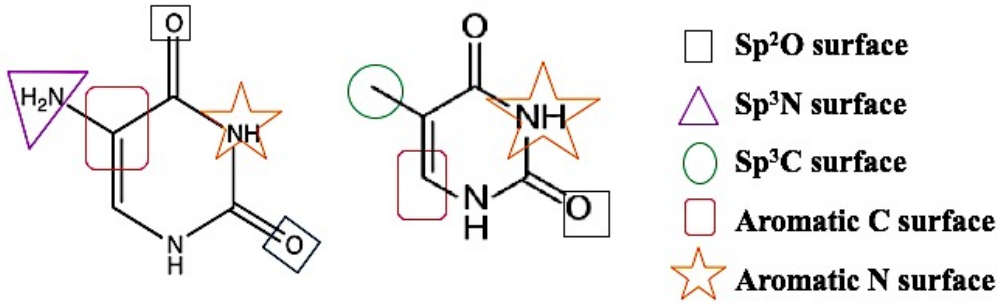

Figure 1. Five types of surfaces that were examined in the analysis (Using Thymine and 5-Aminouracil as examples).

ACKNOLEDGEMENTS

Biggest thanks to Professor Tom Record for accepting me during my freshmen year allowing me to work in his lab for 3 years. Without his help, this project would not be possible and I would not be able to have adequate amount experience to pursue a career in science.

Thanks to Sherry Lixue Cheng for introducing and mentoring me to this project and helping me a lot in data analysis and troubleshooting.

Thanks to Yao Yao for collaborating with me for solubility project.

Thanks to Dr. Ben Knowles, Dr. Irina Shkel, Michael Kerins, and Yurun Zhang for their contributions to this project.

Finally, thank you to Hilldale Committee for providing funding that allowed me to spend more time in lab doing research.